

Undergraduate Demonstration of a Hall Effect Thruster: Self Directed Learning in an Advanced Project Context

Braden K. Oh, Justin H. Kunimune, Lauren M.

Anfenson, Jonah S. Spicher and Rebecca J. Christianson*

Franklin W. Olin College of Engineering, Needham, MA, 02492

(Dated: May 25, 2021)

Abstract

The Hall Effect thruster (HET) is a type of electric propulsion with wide application for in-space propulsion, from satellite station-keeping to deep space travel. Beginning without experience in electromagnetism and plasma physics, we detail our learning process for the physics concepts and principles necessary for a fundamental understanding of electric propulsion and how we applied that learning to the design, manufacture, and successful test-fire of a small, low-power HET. This was accomplished by a team of undergraduates with limited resources for funding and fabrication and was completed within a single semester. As such, we present a path of feasibility for undergraduate electric propulsion projects as a novel vehicle for introductory physics and a case study of an advanced self-directed project at the undergraduate level, outside the context of a traditional research lab.

I. INTRODUCTION

A. Hall Effect thrusters

Traditional chemical rockets generate a large magnitude of thrust over a relatively short time scale, and thus find common usage in launch vehicles, which require high thrust but for only minutes at a time. These chemical rockets, however, are inefficient in space, where large changes in velocity are often required, the thrust can be much lower, and the cost of fuel mass increases exponentially.

An alternative form of thrust is electric propulsion; rather than accelerating molecules through combustion, electric thrusters ionize individual atoms that are then accelerated to extremely high speeds by electric fields. These thrusters generate very low magnitudes of thrust (typically on the order of milli-Newtons), but require substantially less fuel mass per unit impulse and can continue to fire as long as a potential difference can be maintained, sometimes as long as thousands of hours. Ultimately, electric thrusters are capable of achieving large changes in velocity with much less fuel than a chemical rocket, opening doors to highly ambitious space missions—from outer-planet studies to asteroid redirection—and finally make realistic the prospect of human spaceflight beyond lunar orbit.

The Hall Effect thruster (HET) is one such method of electric propulsion that has various advantages over other ion thrusters. Gridded ion thrusters are conceptually simpler devices, but are inherently space-charge limited: positive charges build up between the two plates of a gridded ion thruster, eventually reaching a density that prevents further positive ions from entering the region. As a result, the thruster becomes thrust density limited. HET plasma, on the other hand, remains quasi-neutral throughout the entire ionization region, enabling HETs to avoid this limit.¹ This allows HETs to eventually reach higher thrusts than gridded ion thrusters, and is one of the reasons that we decided to focus on the HET.

Modern research of HETs revolves around thrusters built by graduate students and professors in order to advance the state of the art by improving their efficiency,² developing more accurate simulations of them,³ or bettering our understanding their mechanisms.⁴ This project, however, considers HET not only as a means of electric propulsion but as a tool to learn introductory concepts that HET operating principles are based on, such as plasma physics, electricity, and magnetism. We identified the HET as a potentially apt candidate

for an educational self-directed project because it is so complex and rarely studied at an introductory level, but provides an opportunity to apply many introductory-level concepts.

B. Self-directed project

Project-based learning has become a popular method for improving engagement and efficacy in physics and engineering education,^{5, 6, 7} particularly with respect to technically complex projects as motivation for students to learn abstract concepts. However such projects are rarely initiated, designed, and completed by students, despite the demonstrated efficacy of self-direction.⁸ Such a project is presented in this paper.

This project is both student-initiated and student-led; we decided to undertake it out of an interest in space technology and a curiosity with the challenges of electric propulsion. Some team members had previously interned at NASA JPL and had engaged in projects tangentially related to space propulsion but none had direct experience with electric propulsion beforehand. Instead, the team members had a general interest in electric propulsion and specific interests in the various physics involved with the technology. Our team ultimately engaged faculty to advise the project outside of our regular coursework. As such, we present our path to completing a self-driven, technically-involved project with no prior experience needed for success.

Initially, the scope of the project was to learn physics principles behind electric propulsion, to develop computational modeling skills by modelling electric and magnetic fields, and to apply the theoretical physics from this study (supplemented by material from the standard engineering curriculum) to real thruster design decisions. As the project progressed, however, we developed skills in many fields beyond those we initially set out for, including CAD modeling, design for manufacturing, fabrication limitations and techniques, and interaction with external manufacturing facilities. We also incidentally gained experience with literature searching, as, out of necessity, we sought out and compiled sources of information on electric propulsion and eventually interfaced directly with experts in the field. This process allowed us to realize the potential of projects like these for application-based education: because it was self-driven, we were intrinsically motivated to learn all of these concepts out of necessity.

The core team consists of four undergraduate students from the Franklin W. Olin College of Engineering with academic advisement from Rebecca Christianson, Associate Professor

of Applied Physics. Olin is a 4-year undergraduate school with a focus on project-based engineering curriculum, in which students constantly apply the skills and techniques learned in a classroom to technology demonstrations, rather than exams. As part of this, Olin actively encourages independent studies and academic side projects, and awarded our team general engineering credit for this endeavor.

However, because Olin is relatively new and electric propulsion is a niche field, we were limited in the resources we had available to us. There is no electric propulsion research lab at Olin, no faculty with specific expertise in space propulsion, relatively limited machining capacity (the machine shop houses CNC mills and manual lathes), and we were given no official funding by the school. As a result, it was advantageous for us to optimize our design for simplicity of manufacturing as well as cost. This lack of resources also pushed us to seek outside sponsorship, which was a key component of the success of this project and served as a learning opportunity in itself. In this paper, we aim to provide clarity for the process of designing and building a small, low-power HET in a way that we believe can be generalized to projects that are similar in complexity and scope, as well as document the educational benefits of such an endeavor.

II. LITERATURE SEARCH

Identifying key resources that would give us a background in HET operation, both conceptually and quantitatively, was a critical starting point as neither our team nor anyone else at Olin had previous experience with electric propulsion. We became aware of electric propulsion researchers at NASA JPL who directed us toward the book “Fundamentals of Electric Propulsion: Ion and Hall Thrusters,” which was written by their colleagues Dr. Dan Goebel (JPL) and Dr. Ira Katz (JPL).¹ This is a textbook-like publication that describes key operating principles and provides equations and explanations for determining critical design quantities such as the Larmor radius (see section IV A).

As a second avenue of literature search, we sought out publications from other teams who had previously built demonstration HETs; we were aware of a graduate level class at MIT that had constructed electric thrusters in the past and wanted to know whether this was a common technology demonstration that has already-published literature. We discovered that this is likely not the case, as we could find only one technical report outlining such an

attempt. Matthew Baird published a senior design thesis titled “Designing an Accessible Hall Effect Thruster” while studying at Western Michigan University.⁹ This paper provided a walkthrough of Baird’s high level equations (which matched equations provided by Dr. Goebel) and the design process for a simple HET. Most of the paper was specific to his particular design, and so we used the Baird paper as a case study in applying the methods from Dr. Goebel.

We also sought out present experts in electric propulsion to field project-specific questions. Two individuals who helped us greatly were Dr. Steve Snyder (JPL) and Prof. Manuel Martinez-Sanchez (MIT) who graciously fielded questions from us throughout the process. Our workflow involved reading literature, taking notes, making approximations to verify orders of magnitude, and then developing a list of questions and clarifications for things we did not understand. Each time we amassed a large number of questions, Drs. Snyder and Martinez-Sanchez met with us to answer them. Prof. Martinez-Sanchez also offered feedback as a member of our design review committee before we began manufacturing. We also relied heavily on MIT graduate student Bjarni rn Kristinsson, who interfaced between us and MIT’s test facilities, provided us a hot cathode design, and provided feedback as a member of our design review committee.

The final key piece of literature we relied upon was the Ph.D. thesis “Theoretical and Experimental Investigation of Hall Thruster Miniaturization” by Dr. Noah Warner (JPL),¹⁰ which was recommended by Dr. Martinez-Sanchez. This paper was a full detailed design and analysis of a 9-mm HET developed by Dr. Warner while a Ph.D. student at MIT. Complete with dimensions and an assembly diagram of the full thruster, the Warner paper became a critical reference as we designed our own hardware. Ultimately, our magnetic shunt was nearly identical to Dr. Warner’s design with geometries scaled up by a factor of two.

In identifying and utilizing these resources, we rapidly learned how to conduct research across various mediums including self-studying from textbooks, reading technical papers, and directly contacting and interacting with experts in the field. This process was particularly interesting as we had not been introduced to the concept of a literature search in our coursework, and only recognized it as a ‘literature search’ retroactively. The entire process felt very organic, with the identification of one source or contact leading to the acquisition of several more. Thus, our literature search, which is generally described as a rigid or

structured process, was in reality much more fluid and continued throughout the duration of the project.

III. BACKGROUND INFORMATION AND OPERATING PRINCIPLES

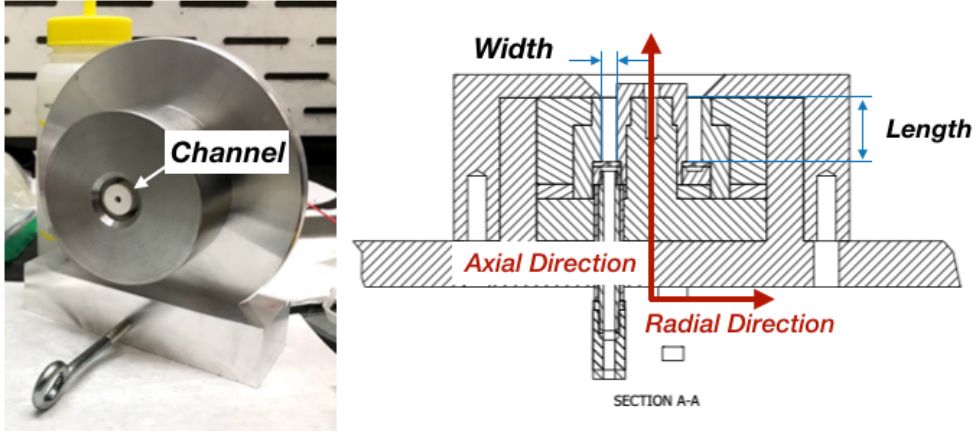


FIG. 1. Labeled diagram of an assembled HET. Left is a photo of our assembled thruster. Right is a CAD drawing of a channel cross section. The channel is the circular cavity in the center of the thruster. The channel width is the width of this cavity in the radial direction. The channel length is the depth of the channel in the axial direction.

The body of a HET, depicted in fig. 1, is cylindrical, with an annular cavity cut into its face. This cavity is called the thruster channel. The radial width of the channel is referred to as channel width, and the axial depth is called channel length. The channel comprises four regions, depicted in cross-section in fig. 2, which govern the thrust generation:

1. the anode, the positively-charged plate at the bottom where gas enters the channel,
2. the ionization region, where the neutral atoms are ionized,
3. the exit plane, where the channel opens into the space above the thruster, and
4. the acceleration region, where ions from the plasma are accelerated to high speeds.

Much of the understanding needed to design a HET revolves around plasma physics—the dynamics of highly ionized gasses—which itself arises from the intersection of electromagnetism and fluid dynamics. In a plasma, there are several kinds of particles in varying

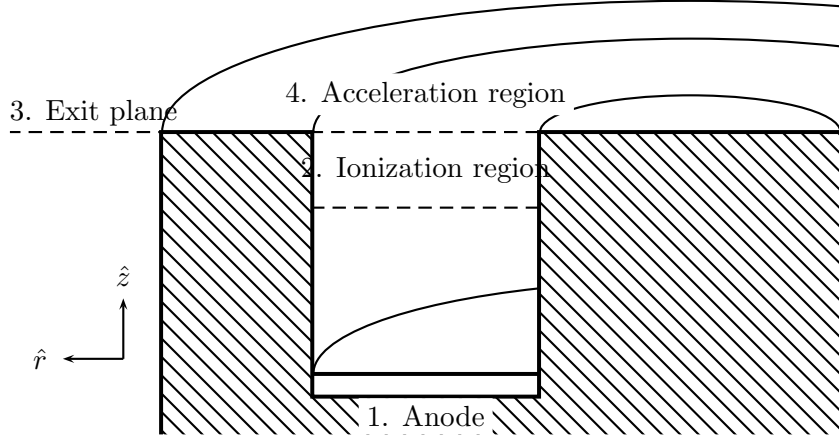


FIG. 2. Cross sectional diagram of the thruster channel with various regions of the channel labelled, as well as the radial and axial coordinates \hat{r} and \hat{z} . These regions are not to scale.

quantities that have different masses and charges: electrons, ions, and neutrals. Each particle individually follows a fairly simple equation, Newton's law applied to an electric field \vec{E} and magnetic field \vec{B} (gravity and other forces can usually be neglected),

$$m\vec{a} = q\vec{E} + q\vec{v} \times \vec{B} \quad (1)$$

This manifests by causing positive charges to accelerate along electric fields and circle around magnetic fields, and negative charges to do the same, but in the opposite direction. The radius with which particles gyrate around magnetic field lines is known as a Larmor radius, or gyroradius. The Larmor radius of the charged particles in the thruster channel provides a major design constraint when determining the channel dimensions.

The electromagnetic fields are then governed by Maxwell's equations:

$$\nabla \cdot \vec{E} = \frac{\rho}{\epsilon_0} \quad (2)$$

$$\nabla \times \vec{E} = -\frac{\partial \vec{B}}{\partial t} \quad (3)$$

$$\nabla \cdot \vec{B} = 0 \quad (4)$$

$$\nabla \times \vec{B} = \mu_0 \vec{J} + \mu_0 \epsilon_0 \frac{\partial \vec{E}}{\partial t} \quad (5)$$

The first two tell us that electric field lines point from positive charges to negative charges, and are thus characterized by their direction and divergence, while the final two tell us that magnetic field lines form closed loops around electric currents and are thus characterized by their curl.

When a plasma interacts with an insulative charged object, the charges in the plasma move to surround and thus “screen out” the object from the rest of the plasma. For example, when a positively charged object comes into contact with a plasma, negative particles from the plasma gather around its surface, while positive particles move out of its vicinity. This results in a locally negative surface covering the positive surface, which in turn attracts its own, weaker, layer of positive charges. These alternating layers of weakening charge that surround a charged object are known as a Debye sheath, or simply a sheath. This sheath blocks the electric field emanating from the object such that the object has no electric influence far beyond its sheath, a process known as screening. The screening of the anode by the plasma in the channel causes the voltage drop up to the ionization region to be very small, inducing a large voltage gradient near the exit plane and resulting in a distinct acceleration region of the channel. This allows the positive ions to be rapidly accelerated out of the thruster.

Electric thrusters generate ions from an inert propellant and accelerate these ions with a strong electric field. The HET generates ions by trapping high-energy electrons within a circular channel into which the propellant is injected. As the propellant atoms move through the channel, they pass through this cloud of trapped electrons and experience collisions which impart enough energy to remove an electron from the propellant atoms, a process known as electron bombardment. The result of this electron bombardment is a plasma.

At the base of the channel an anode is charged to a few hundred volts relative to a cathode that lies outside of the thruster. This results in an electric field within the channel, which aligns with the axis of the thruster, perpendicular to the anode, due to the dielectric material that surrounds the channel walls. This field reaches through the channel and out of the the thruster to terminate at the cathode. This field accelerates the positively charged plasma ions away from the anode and into space, generating forward thrust by conservation of momentum.

Electron trapping occurs with the help of a radial magnetic field that peaks at the exit plane of the thruster. When electrons from outside the channel first cross the exit plane and enter the channel, they have velocity in the axial direction (i.e. they are being accelerated down into the channel by the electric field). In the orthogonal electric and magnetic fields, the electrons experience $\vec{E} \times \vec{B}$ drift in the azimuthal direction. This drift arises from the cycloidal motion charged particles naturally exhibit in such fields; a general example of such

drift is illustrated in fig. 3. In a HET, this azimuthal drift causes them to travel circularly through the channel, as illustrated in fig. 4. As atoms of the injected propellant pass through this swirling cloud of electrons they are bombarded by the electrons and form a plasma.

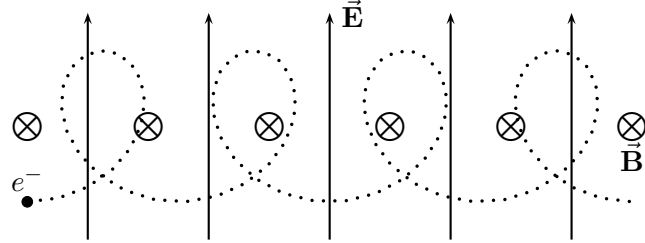


FIG. 3. The cycloidal trajectory of an electron undergoing $\vec{E} \times \vec{B}$ drift in a uniform electric and magnetic field. The electron tends to circle counterclockwise in the magnetic field, but the electric field imposes an additional constant acceleration that causes it to travel faster at the bottom of the circle. The net result is a constant rightward drift velocity.

Outside of the thruster, a cathode generates the high-energy electrons necessary to ignite the thruster and neutralize the thrust plume. Igniting a HET proves difficult because enough electrons must be trapped to facilitate collisions with propellant atoms and those electrons must also have enough energy to overcome the work function of the propellant. Once an initial plasma is formed, a cascade effect occurs as the electrons newly freed by plasma formation are themselves able to collide with yet more propellant atoms, and so forth. In a hot cathode, high-energy electrons are generated by creating this initial plasma; a small amount of propellant gas is heated in a chamber until the element’s work function is overcome and a plasma forms. A keeper plate outside of the chamber is positively charged so as to draw released electrons out of the chamber.

The “lifetime” of an electron in this setup is as follows: a neutrally charged propellant atom is injected into the hot cathode, where it is heated and an electron is freed from it.

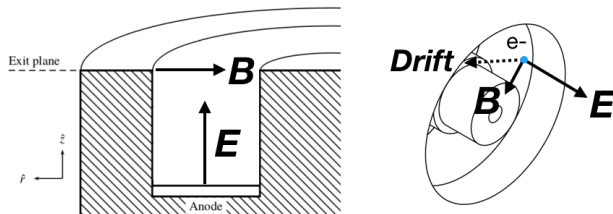


FIG. 4. The directions of the electric and magnetic fields in the channel.

The free electron experiences an electric field between the cathode body and keeper plate, drawing it out of the cathode body and into free space. It then either is attracted into the positively charged thrust plume, or follows the electric field between the cathode and thruster anode into the channel. If it enters the plume, it neutralizes positive ions within and leaves the system. If it enters the channel, the electron experiences a radial magnetic field along with the electric field, which causes it to undergo azimuthal drift. This electron travels in a cycloidal path inside the channel—circular because of the magnetic field but falling ever closer to the anode due to collisions with other electrons. It may collide with ions while circling the ionization region, ionizing them, scattering more free electrons, and possibly being pushed out of the channel. Otherwise, it will eventually strike one of the walls and be absorbed, eroding them slightly in the process.

IV. HALL THRUSTER DESIGN

Developing the thruster required major design decisions in five main areas: (A) the magnetic field, (B) the channel, (C) the anode (electric field), (D) the cathode (initial plasma source), and (E) materials. The magnetic and electric fields determine how electrons behave within the channel, the dimensions of the channel determine the amount of plasma generated and the chance of its particles colliding with the walls or anode prematurely, and the hot cathode ensures both closure of the electric field and an initial source of high-energy electrons to aid in thruster ignition. Naturally, the materials used throughout also have various effects on efficacy, and chance of failure by cracking, demagnetizing, or eroding.

The process of designing a system both to meet design constraints and to be within capabilities of manufacture synthesized skills and techniques from many of our previous classes.

A. Magnetic Field Design

The magnetic field has four major constraints:

1. The field must be radial. A strong radial field combined with the axial electric field ensures that electrons entering the channel experience azimuthal drift and become trapped within the channel. If the magnetic field has too weak of a radial component,

electrons will rapidly fall into the anode, inhibiting the thruster’s ability to ionize propellant.

2. The field must peak in strength at the exit plane. This allows the thruster to trap electrons just as they enter the channel and results in a concentration of electrons just below the exit plane. If the field strength is too uniform in the axial direction, or if it peaks elsewhere in the channel, the electrons will not concentrate highly enough to cause sufficient collisions with neutral propellant.
3. The field must be strong enough to trap electrons. To this end, the field must be strong enough to ensure that the electron Larmor radii are significantly smaller than the length of the channel. If the field is too weak, highly energetic electrons will escape the ionization region. This results in a higher rate of collisions between electrons and the channel walls, reducing the number of electrons available for propellant ionization.
4. The field must be weak enough to not trap ions. The field must be weak enough to ensure that the ion Larmor radii are significantly larger than the length of the channel. If the field is too strong, ionized propellant will become trapped in the ionization region rather than accelerating outwards, and the thruster will generate no thrust.

Constraints 1 and 2 are typically achieved in one of three ways: with electromagnets, with a radially-aligned permanent magnet, or with an axially-aligned permanent magnet with a “shunt” that controls the strength and direction of the magnetic field near the exit plane. Due to the high current draw of electromagnets and the high price of radially-aligned magnets, we decided to use the third approach, the magnetic shunt: six permanent samarium cobalt (SmCo) magnets were embedded in a specially shaped piece of iron. Iron was chosen for its strong ferromagnetic response (see subsection IV E). The initially non-magnetic shunt, depicted in fig. 5, experiences a ferromagnetic response to the SmCo magnets. This guides the magnetic field to be both radial and peaking in strength just below the exit plane by a geometry that draws the magnetic field radially through a lip in the outer edge of the channel and across the channel into a core inside the channel. Our shunt geometry was pulled directly from the Warner paper¹⁰ and scaled by a factor of two. Fig. 6 shows a COMSOL model of the shunt assembly and the predicted resulting field. The 6.35 mm diameter SmCo disk magnets we decided to use had magnetizations of 10.4 kG, which COMSOL predicted would

result in a peak radial field strength of 28.0 mT. The actual peak strength, as measured by a handheld Hall probe, turned out to measure between 22.5 mT and 25.6 mT .

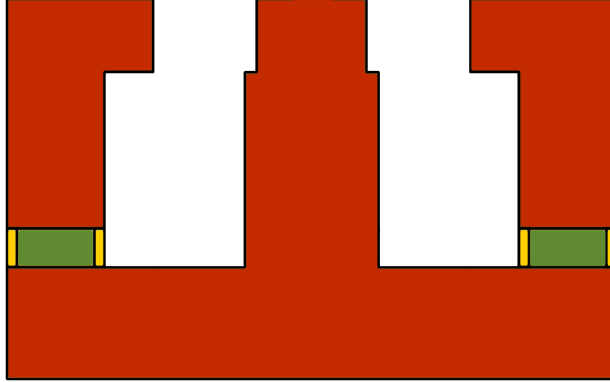


FIG. 5. Cross section of the magnetic shunt. The iron shunt is depicted in red, the SmCo disk magnets are depicted in green, and the aluminum magnet retaining ring is depicted in yellow.

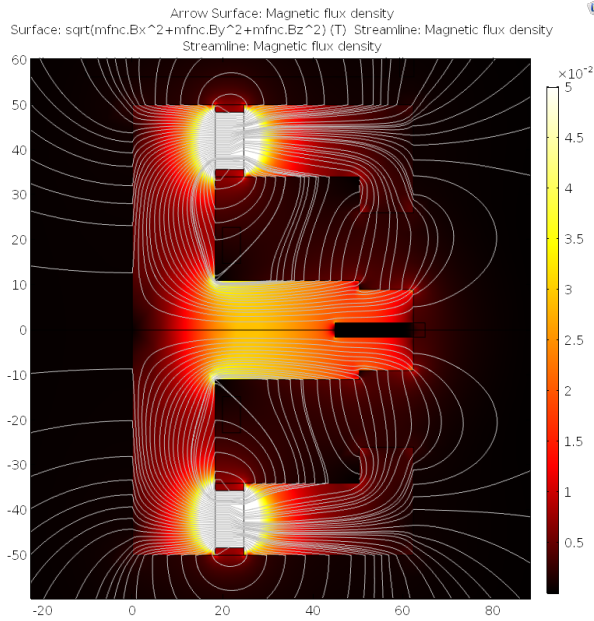


FIG. 6. Predicted magnetic field inside the shunt. Lines are magnetic streamlines, and color is total magnetic field strength. There is no predicted or measured azimuthal magnetic field.

Constraints 3 and 4 are met by fixing the anode voltage and by setting the channel size to be between the resulting Larmor radii. The relationships between Larmor radius, field strength, and operating voltage are given by the following equations, provided by the Goebel

book:¹

$$r_e = \frac{1}{B} \sqrt{\frac{8m_e T_{\text{eV}}}{\pi e}} \quad (6)$$

$$r_i = \frac{1}{B} \sqrt{\frac{2m_i V_b}{e}} \quad (7)$$

where r_e and r_i are the Larmor radii of an electron and ion respectively, B is the magnetic field strength, m_e and m_i are the masses of an electron and ion respectively, T_{eV} is the average kinetic energy of an electron in eV, and V_b is the potential drop that the ions are accelerated across. To perform these calculations we relied upon the following values: 2.80×10^{-4} T for B , as predicted by the COMSOL magnetic field model; 350 V for V_b , an arbitrary value that is on the same order of magnitude as the Baird thruster,⁹ which operated at 300 V and is within the operating voltage achievable by power supplies at the MIT Space Propulsion Lab; and 35 for T_{eV} , as the Goebel book stated that one tenth of the operating voltage is a reasonable estimate for electron temperature.¹

Using these values, we computed $r_e = 0.83$ mm and $r_i = 610$ mm. These radii determine that the channel length must be significantly higher than 0.83 mm and significantly lower than 61 cm in order to both trap electrons and free ions. As 61 cm is a very large dimension on the scale of this thruster, the constraint that matters most is r_e . The Goebel book asserts that a reasonable channel length is at least five times longer than the electron larmor radius.¹ To this end, the minimum channel length should measure 4.15 mm. The range set by these this minimum length and r_i varies by two orders of magnitude and falls comfortably within manufacturable dimensions. Given these reasonable design parameters, we were content with the strength of our magnetic field and continued with the design process.

B. Channel Design

The channel was designed with five major considerations in mind:

1. The channel length should be significantly longer than the neutral mean free path length. The neutral mean free path is the average distance a neutral particle will travel before experiencing an ionizing collision with an electron. If the channel length is too shallow, neutral propellant will exit the channel without ever being ionized, resulting in greatly reduced thrust.

2. As stated in the previous section, the channel length should be significantly longer than the electron Larmor radius. If the channel is too shallow, gyrating electrons will quickly reach the anode and reduce the number of electrons available for propellant ionization.
3. As stated in the previous section, the channel length should be significantly shorter than the ion Larmor radius. If the channel is longer than the ion Larmor radius, ions will circle back into the channel instead of escaping and no thrust will be generated.
4. The channel geometries should fall within a range of reasonably manufacturable dimensions and tolerances. Olin College has manufacturing capabilities geared towards large projects (e.g. Formula and Baja racing vehicles) rather than small ones, and too small of a geometry would prove difficult to manufacture in-house.
5. The channel walls should be made of a material that is electrically insulative while remaining as thermally conductive as possible. The walls must be electrically insulated to prevent the plasma from shorting to ground through the metal components of the shunt. The thermal consideration was made because the plasma's high temperature could potentially damage nearby thruster components if not properly transported, and heat must be conducted away from the plasma by the channel walls due to the surrounding vacuum.

To meet the first constraint, we first estimated the neutral mean free path length using the following equation provided by Goebel:¹

$$\lambda = \frac{v_n}{n_e \langle \sigma_i v_e \rangle} \quad (8)$$

where λ is the mean free path, v_n is the velocity of the neutral particles, n_e is the electron density, and $\langle \sigma_i v_e \rangle$ “is the ionization reaction rate coefficient for Maxwellian electrons.¹” We did not know enough about our propellant supply or the dynamics inside the channel to precisely calculate v_n , n_e , or $\langle \sigma_i v_e \rangle$. However, we were able to make educated estimations for each.

For the neutral speed, we used the thermal speed of the propellant gas. The flow rate, which would determine the average neutral speed through the channel, would likely be much lower as thermal speeds are usually much higher than fluid speeds. However, this high

estimate was easier to compute, and gave us more conservative channel size. Assuming the propellant was at room temperature, this speed would be

$$v_n \approx v_{\text{th}} = \sqrt{\frac{2kT}{m_{\text{Ar}}}} = 350 \text{ m s}^{-1} \quad (9)$$

For the electron density, we assumed the electrons to be an ideal gas at standard pressure and the aforementioned estimated temperature of $35 \text{ eV} = 4.1 \times 10^5 \text{ K}$. This corresponds to a number density of $1.8 \times 10^{22} \text{ m}^{-3}$. This was on a similar order of magnitude to electron densities described in Goebel.¹

The ionization rate could be determined only through empirical tables. Chung *et al.*¹¹ had already published such rates for argon, so we simply looked up the value corresponding to the electron temperature most like what we expected to see during operation: around 35 eV (rounded to the nearest value present in Chung *et al.*'s table, 32 eV). This value was $3.112 \times 10^{-14} \text{ m}^3 \text{ s}^{-1}$. With these values in place, the mean free path came out to $\lambda = 630 \text{ nm}$. Given that this is much smaller than the previously computed electron Larmor radius of 0.83 mm , as long as the electron trapping constraint is met, the mean free path constraint is automatically met as well, ensuring that nearly all of the propellant should ionize before leaving the channel.

Constraints 2, 3, and 4 were all met by selecting a channel length of 16 mm which both fell between 0.83 mm and 61 cm and fell comfortably within the manufacturing capabilities of Olin's machine shop. Furthermore, it established a dimension that could fit comfortably within the magnetic shunt geometry while still accommodating the thickness of the anode and its insulating material. Constraint 5 was met by manufacturing the channel walls of a boron nitride ceramic. An explanation of this material decision is given in section IV E.

The final necessary channel dimension is the width. Ultimately the width of the channel sets the final ratio between volume and surface area. A channel with a very low ratio will have a dense plasma, but will lose many charged particles to collisions with channel walls. A channel with a very high ratio will lose many fewer particles to wall collisions, but will have a low plasma density. As such, the channel width must be low enough to achieve a high plasma density while remaining as large as possible to reduce the number of wall collisions. To determine this value we relied upon the following law provided by Baird:⁹

$$w = r_{\text{out}}(1 - k) \quad (10)$$

where w is the channel width, r_{out} is one-half of the outer channel wall diameter (i.e. the radial distance between the center of the thruster and the outer wall), and k is a scaling constant. The SPT-100, an extensively studied HET with extensive flight heritage, has 0.7 as its scaling constant.⁹

The calculation for width cannot be closed, however, without first determining a value for r_{out} . Our shunt geometry was the same as the shunt used by Warner¹⁰ scaled by a factor of two. This shunt, when assembled, had a cavity to accommodate the final channel that was considerably larger than it needed to be. We decided to center our final channel within this cavity: the largest available radius for the final channel was 13 mm, and the narrowest available radius was 5.5 mm. The average of these two values is 9.25 mm, so we determined to center the channel about that radius.

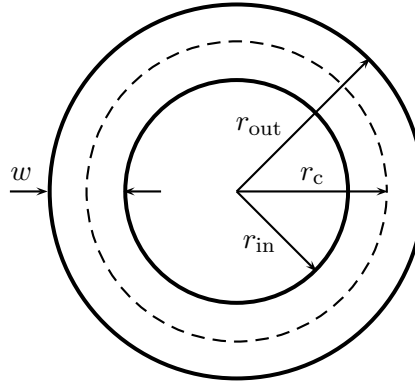


FIG. 7. Diagram of the thruster channel geometry viewed axially, as though looking down into the channel. The solid circles represent the inner and outer walls of the channel and have radii given by r_{in} and r_{out} , respectively. The dotted circle is an imaginary circle that marks the center of the channel and has radius r_c , which measures 9.25mm for our thruster. The width of the channel is the distance between the inner and outer walls and is given by w .

The measures of the inner and outer walls are related by the width

$$r_{\text{in}} + w = r_{\text{out}} \quad (11)$$

and we will refer to the mean of r_{in} and r_{out} as r_c . Solving equations 10 and 11 for r_{out} yields the following equation for r_{out} :

$$r_{\text{out}} = \frac{2r_c}{1+k} \quad (12)$$

As r_c and k are known to be 9.25 mm and 0.7 respectively, the radius of the outer channel wall is given by substitution to be 10.88 mm. With this value for r_{out} , the channel width can now be determined with equation 10 by substitution to yield $w = 3.26$ mm.

C. Anode Design

The physical design of the anode is constrained only in that it must be made from a conductive material that can hold a high voltage and can withstand exposure to the energetic plasma. In addition, it is convenient for the propellant injection system to be incorporated into the anode. Most dimensions of the anode are determined by the dimensions of the channel.

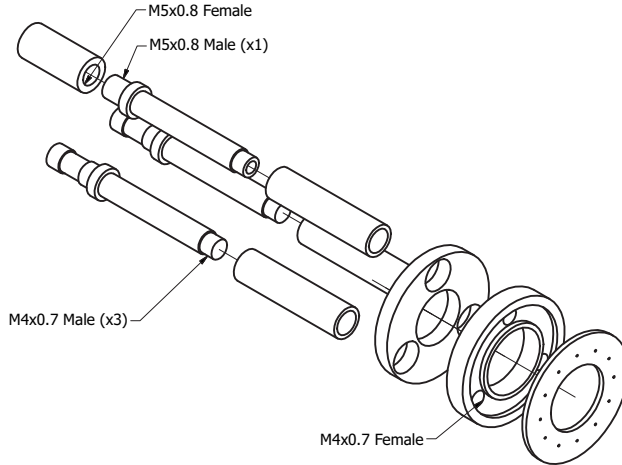


FIG. 8. An exploded diagram of the anode, with the direction of propellant flow down and to the right.

Our anode consists of a disk set at the bottom of the thruster channel and is held at a high positive electric potential relative to the (external) cathode. The high voltage of the anode generates an axial electric field that both draws electrons into the channel and accelerates the ionized propellant out of the channel.

There are two anode shapes that are commonly used in HET: the first consists of a flat ring in the bottom of a channel with dielectric walls; the other consists of an anode that

extends up onto conductive channel walls. The latter, with conductive walls, enables the walls to be negatively biased, repelling the electron plasma toward the center of the channel. However, the extended anode that this requires is then closer to the hot plasma and thus more prone to damage. The former, with the dielectric walls, is more common and simpler to manufacture. Given that we planned to manufacture the majority of our parts in-house with the machines that we had available to us, and none of these offered the capability to machine the fine details that a metal-walled thruster would require, we chose the former flat ring anode design.

The anode hardware also serves to inject propellant into the channel. This is done in a method similar to that of the Baird thruster,⁹ which in turn resembles the method used to distribute air evenly across an air hockey table. A thin steel disk with 12 holes drilled through its face, shown in the lower right of fig. 8, is laid atop a thicker steel disk with a channel carved into its surface. Gaseous propellant is fed into this anode channel underneath the thin disk by means of a small pipe, and the propellant expands to fill the volume of the anode channel. So long as the holes in the thin disk are sufficiently small, the propellant in the anode channel will pass through all the holes relatively equally and so will fairly evenly diffuse into the thruster channel.

To achieve the pressure difference between the anode channel and thruster channel necessary to attain an adequate diffusion of propellant, we determined that the area of the holes in the thin plate (the exit area of the propellant) must be significantly smaller than the area of the pipe that the propellant is pumped in through. This is done in order to restrict the flow of propellant out of the anode just enough to build up approximately uniform pressure inside the anode channel, and thus an approximately equal pressure behind each outflow hole. We arbitrarily set this ratio between the outflow area and the inflow area to 4, enabling us to solve for a numeric outflow hole diameter:

$$A_{\text{in}} = 4A_{\text{out}} \quad (13)$$

$$\frac{1}{4}\pi d_{\text{in}}^2 = 4N \frac{1}{4}\pi d_{\text{out}}^2 \quad (14)$$

$$d_{\text{out}} = \sqrt{\frac{d_{\text{in}}^2}{4N}} \quad (15)$$

where A_{in} is the cross sectional area of the inflow pipe, A_{out} is the total cross sectional area of the outflow holes, d_{in} is the diameter of the inflow pipe, d_{out} is the diameter of a single outflow hole, and N is the total number of outflow holes. The diameter of our inflow pipe was 2.5 mm and we chose to drill 12 outflow holes, allowing us to solve for an outflow hole diameter of 0.4 mm. Although 0.4 mm is a standard drill bit size, the Olin College machine shop did not carry such a drill bit, requiring us to cut the holes by only partially plunging the tip (which is a 118° point) of the smallest available drill bit through the thin anode disk. This method of manufacturing understandably resulted in an enormous lack of precision, and so the actual diameter of the diffuser holes varied greatly.

External access to the anode was provided by three holes drilled through the back of the thruster assembly and into the anode. These holes fully penetrated the bottom of the anode to provide access to the anode channel. Three steel “legs”, shown in the upper left of fig. 8, were screwed into these holes and protruded through the back of the thruster. Two of these legs were solid all the way through and provided a reliable point of electrical connection to the thruster. The third leg was drilled through the center and served as a pipe through which propellant could flow from an exterior source into the anode channel. This gas feed tube was male threaded at the protruding end and screwed into an aluminum adapter that allowed an interface between the gas feed tube and a 6.35 mm NPT fitting. The MIT Space Propulsion Laboratory (SPL) vacuum chamber gas feed system connected to this adapter through a 6.35 mm male Swagelok connector.

All three legs were sized to fit inside ceramic sheaths that served to electrically isolate each leg from the rest of the thruster body, as the legs would necessarily become charged to the same potential as the anode. These sheaths were made from alumina ceramic tubes bought off-the-shelf from McMaster-Carr.

D. Cathode Design

The hot cathode provides a source of electrons to sustain a plasma inside the thruster as well as to neutralize the thrust plume during firing (else the thruster builds up a net negative charge to which the positive ions return and negate the generated thrust). At the center of the cathode is a cavity into which a small amount of propellant gas is injected. A thin wire inside this cavity is strung between two electrodes across which a voltage is

applied. The resultant electrical current heats the wire, which in turn ignites a plasma in the surrounding propellant, generating positive ions and free high energy electrons. An external metal plate called a keeper plate, which is electrically isolated from the rest of the cathode, is then charged to a positive potential relative to the cathode body and draws a negatively charged plasma out of the cathode. The high energy electrons inside this plasma are then drawn down into the thruster channel. In addition to aiding in initial thruster ignition, these electrons form a plasma bridge that can conduct current and enable electrons to flow freely through the space between the thruster and cathode that would otherwise be a vacuum.

While the thruster is firing, a positively charged thrust plume is emitted. During thruster operation, the cathode continues to emit a net negative plasma which conducts through the aforementioned plasma bridge and is either drawn down into the thruster channel, aiding in propellant ionization, or is drawn into the positively charged plume, effectively neutralizing it.

We selected a 0.102 mm tungsten filament for the heater wire because of its high melting point and relatively high electrical resistivity. Because it is relatively resistive, the thin filament was easy to heat with a fairly small current (on the order of a single-digit number of Amps), and because its melting point is very high, the filament could withstand temperatures of over 1000 K without melting. The wire was coiled as tightly as possible and spot welded to stainless steel electrodes. A measurement with a multimeter determined that our filament had a resistance of 3Ω .

The keeper and cover plates were attached by alumina rods and ceramic washers and cemented together by a high temperature ceramic cement purchased from OMEGA Engineering to assure that the plates were held at a constant distance and were electrically isolated. These rods then slid into holes in the cathode body, allowing the cover plate to contact the cathode body and keeping the keeper plate isolated and at a fixed distance from the plasma cavity. A voltage of about 300V was applied to the keeper plate—a high enough potential that the electrons are drawn out of the cathode body, but lower than the anode voltage so that electrons, after being drawn out of the cathode and before the thruster ignites, will be drawn down into the thruster channel.

A CAD view of our cathode is shown in fig. 9, a clearer cross section of the cathode is shown in fig. 10. The design for this cathode was provided by MIT student Bjarni rn

Kristinsson, who had designed a cathode previously for a graduate level course. Kristinsson's cathode design was accompanied by a technical report that provided a handful of lessons learned during manufacturing, and our design followed slight modifications to his to address some of these concerns.

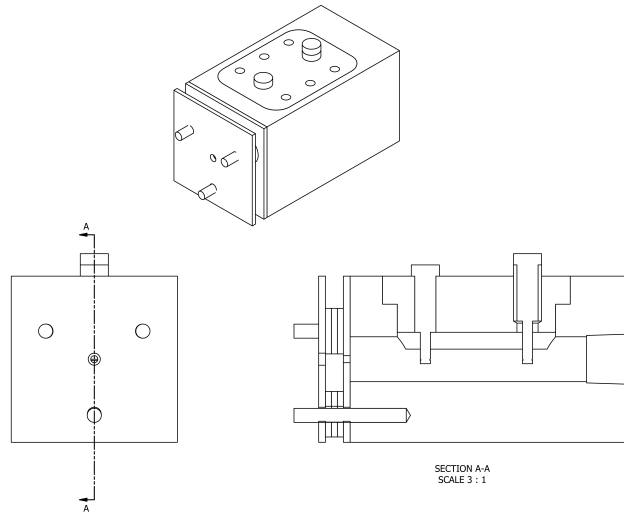


FIG. 9. CAD drawing of the assembled cathode from isometric (top), front (left), and cross sectional (right) views.

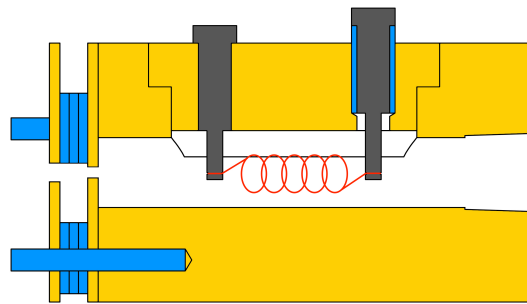


FIG. 10. Enlarged cross section of the assembled cathode. Aluminum components are shown in yellow, ceramic components in blue, steel components in grey, and the tungsten filament in red. The keeper plate is the leftmost aluminum component and is held off from the body of the cathode by ceramic washers.

E. Materials

The HET components were primarily composed of four materials; boron nitride (BN), stainless steel (SS303), iron (ST42-S), samarium cobalt (SmCo), and aluminum (2014 T-6), with the anode legs insulated with alumina (aluminum oxide). The cathode components were composed of scrap aluminum, mild steel, and tungsten filament available at Olin College.

The thruster walls were manufactured from BN, a ceramic material which has the unusual property of being fairly thermally conductive while remaining electrically insulative. BN is a specialty material that is expensive and difficult to acquire; our BN stock was donated generously by Busek Co., an electric propulsion research and manufacturing facility in Natick, Massachusetts. This material would electrically isolate the plasma in the channel from the grounded thruster assembly while remaining able to conduct heat away from the channel and into the rest of the thruster. This property is important because the thruster must be fired inside a vacuum, within which the primary mode of heat flow is conduction between thruster components. Thermally conductive channel walls allow hardware in contact with the channel to conduct heat away as rapidly as possible. Keeping the temperature of the thruster hardware as low as possible is important for two reasons. First, thermal expansion could cause certain components to expand into and crack the components surrounding them. This is of particular concern inside the channel; BN has an extremely low coefficient of thermal expansion, so a highly expanding anode could expand into and crack the channel walls. Second, because the thruster relies on permanent magnets to maintain a magnetic field critical to operation, the maximum operating temperature of magnetic components must not be exceeded.

The anode diffuser plate was manufactured from SS303, a steel alloy with a high chromium/nickel composition (18%/8%, respectively). This is a stainless steel alloy that exhibits a high level of toughness and is routinely used in industrial machines, pumps and valves, and aircraft. We selected SS303 for its ability to withstand corrosion, with the hope that it would withstand the energetic plasma of the thruster channel with minimal erosion or adverse reaction with stray gas and other contaminants present in the testing environment.

The thruster walls were enclosed within a magnetic shunt manufactured in two pieces out of ST42-S, a steel alloy with an iron content of $\geq 99.75\%$. We selected iron for the shunt because of its properties as a soft ferromagnetic material. Its melting point and Curie

temperature are also sufficiently high for the conditions we expected in the thruster. Iron's ferromagnetism is extremely useful because it gives the iron the property of being able to "conduct" magnetic field lines, as the magnetic regions in the iron will align according to an applied magnetic field. To this end, holding a strong permanent magnet near the shunt will cause the shape of the magnetic field to follow the geometry of the steel, allowing us to precisely control the shape and strength of the magnetic field at the exit plane.

The strong magnetic field applied to the shunt was applied by six permanent SmCo magnets purchased off-the-shelf from CMS Magnetics. We selected SmCo for its high maximum operating temperature of 150 °C.¹² In order to hold these magnets at precise locations within the shunt, we designed a 2014 T-6 aluminum retaining ring with six slots to house the magnets. We selected aluminum for this retaining ring because aluminum has an extremely weak ferromagnetic response. Using a ferromagnetic material such as ST42-S for the retaining ring would have amplified the magnetic field in directions that are not conducive to maximizing the radial magnetic field and, according to our COMSOL model, would have severely decreased the magnetic field strength in the ionization region of the channel. The 2014 alloy of aluminum is routinely used in aerospace applications. It exhibits high strength and hardness for aluminum but generally poor corrosion resistance.

The assembled channel and shunt formed the core of the thruster, which was mounted inside of a 2014 T-6 aluminum heat sink. Aluminum was used for the heat sink because it has a high thermal conductivity and is cheap and readily available. Although its heat capacity is not remarkably high, its low cost allowed us to have a large surface area which served to quickly radiate heat into the vacuum test environment.

The core and heat sink were bolted together by a cover also composed of SS303 steel. Again, this stainless steel alloy was selected in the hope of resisting erosion by high energy particles or any unexpected reaction between the cover and stray contaminants on the surface of the thruster or otherwise floating within the test chamber during operation.

Three legs are screwed into the back of the anode and protrude from the rear of the thruster; in order to maintain the anode's electrical isolation, each of these legs were insulated from the rest of the thruster assembly by surrounding them in sheaths of alumina. Alumina is a ceramic material which is non-conductive. The anode legs were sized to fit within an off-the-shelf alumina tube that was cut to length.

F. Manufacturing and Assembly

All components of the thruster would require a 0.5 mm manufacturing tolerance. Olin College has an in-house machine shop, but a number of concerns led us to seek an outside vendor to manufacture the majority of the thruster hardware. If we used the in-house shop, we, as individuals, would need to manufacture all hardware ourselves. Given that we did not have a large amount of manufacturing experience, we were not confident in our ability to consistently meet the required tolerances. Furthermore, the Olin shop has a limited number of machines, and we needed to manufacture a large volume of parts, which would have put us at odds with other students who also required the machines for their own classes and projects. For these reasons, we secured sponsorship from C. Lal Alloys (P) Ltd., a large metal manufacturer in India. We were introduced to this company by Sparsh Bansal, a student at Olin College, with familial ties to the company. Bansal interfaced with the company and negotiated an in-kind donation of material and manufacturing time.

All contacting surfaces were toleranced in opposite directions, such that there would always be a narrow amount of clearance between components. For instance, the widest diameter on the shunt was toleranced to -0.5 mm and the narrowest diameter on the heat sink that the shunt slides inside of was toleranced to 0.5 mm. This guaranteed that the parts would successfully fit together, while minimizing the gap between them. For this reason, rigid connectors between components were not necessary, and all components, when assembled, were held together only by bolts passing through the back of the heat sink into the front cover of the thruster. A color coded cross section of the fully assembled thruster is given in 11.

V. TESTING

Thanks to a generous donation by MIT, we were able to perform tests in the MIT SPL's vacuum chamber using Argon that they provided. We performed three live tests over three days and successfully ignited the thruster with Argon during the second test.

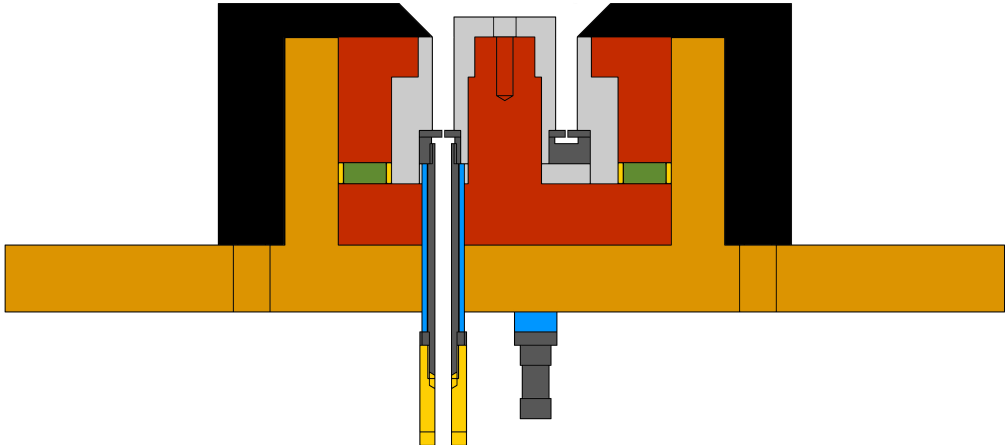


FIG. 11. Cross section of the fully assembled thruster. The front cover of the thruster is shown in black; all other steel components are shown in dark grey. Boron nitride components are shown in light grey. Alumina components are shown in blue. The heat sink is shown in gold; all other aluminum components are shown in yellow. The iron shunt is shown in red. The samarium cobalt magnets are shown in green.

A. Cleaning and Setup

Before testing, all of our components were cleaned to remove stray oils and other contaminants that could potentially off-gas when exposed to a vacuum and cause unexpected reactions during testing. All thruster and cathode parts were washed in an isopropanol alcohol bath before assembly. At MIT, prior to testing, all assembled hardware was surface cleaned an additional time, first with isopropanol and then acetone. All clean hardware was handled with nitrile gloves.

The vacuum chamber is a large cylindrical chamber with a flat, gridded platform inside for mounting hardware to. For the first test we used two test stands, one for the cathode and one for the thruster, shown in fig. 12. The cathode stand was made of copper sheet metal and consisted of a small square platform raised in the air by two legs. The thruster stand was made from aluminum plates stacked upon a structure of 80-20 metal bars.

The cathode body and thruster body were grounded to the chamber wall. Three wires ran out of the chamber; one for the keeper plate voltage, one for the cathode filament, and one for the thruster anode voltage. These wires were hooked up to external power supplies,

which were controlled from outside the chamber. A photo of the test stand setup is given in fig. 12, and a schematic of the electrical setup is given in fig. 13.

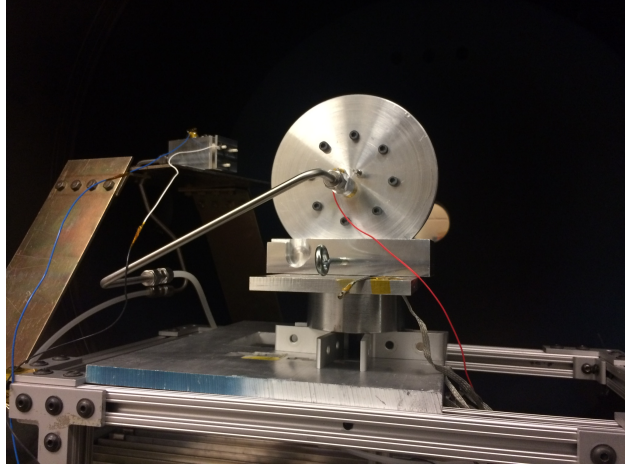


FIG. 12. Image of the cathode and thruster positioned inside the open vacuum chamber prior to the first test. The cathode, visible from the front, is positioned on a copper test stand and points towards the front of the thruster. The thruster, visible from the rear, is positioned atop an 80-20 frame with the channel pointing towards the rear of the test chamber.

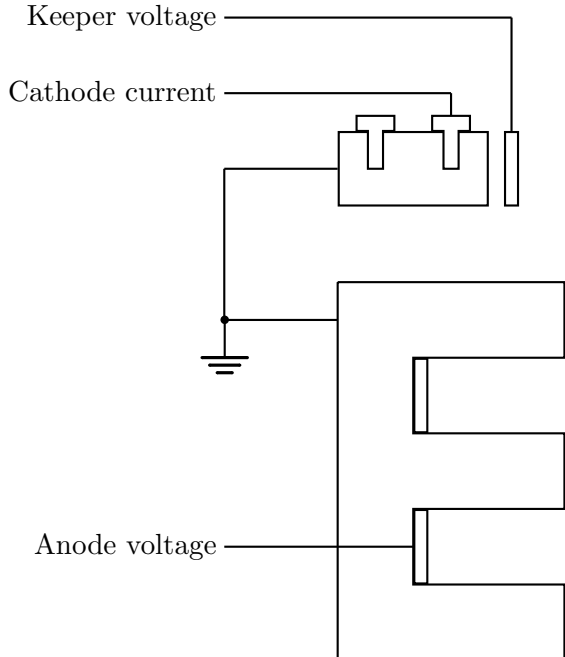


FIG. 13. The electrical layout of our test setup.

B. Successful fire

A plasma plume was successfully observed on the second day of testing. The cathode filament had burned out earlier in the day due to too much sustained current, so the thruster was ignited using only free electrons in the vacuum chamber. When a potential of 450 V was applied to the anode and the propellant flow rate was maxed out at 10.0 sccm, pulsed firing was observed. The pulsing continued, less reliably, as the flow rate was brought down to between 1.33 sccm and 2.07 sccm. At higher flow rates the thruster pulsed regularly at around 5 Hz. An image of a thrust pulse is given in fig. 14.



FIG. 14. Thrust pulses captured from the side (left) and front (right) of the thruster. The pink glow is characteristic of an Argon plasma.

Each pulse was brief and resembled a discharge of static electricity. During each pulse we observed up to three simultaneous flashes of light: a pink plume emerging from the channel, a pink cloud surrounding the gas feed connector at the rear of the thruster, and a white flash near the gas feed connector of the burnt-out cathode. A pink glow is characteristic of an argon plasma. As such, the pink plume emerging from the channel was a sign of plasma being accelerated out of the thruster and was a sign of successful operation. The pink plume emerging from the rear gas feed connector was concluded to be the result of a leaky gas feed connection. We used Swagelok branded tubing and connectors in the gas feed lines; the connector at the rear of the thruster, which interfaced a smooth Swagelok tube to the thruster feed adapter, contained exposed sharp edges on the threads of the connector that did not fully screw into the aluminum thruster feed adapter. This was expected, as the thruster adapter was an NPT type fitting that expects some leftover threading even when

fully tightened, but also resulted in unanticipated concentrations of electric field about those sharp edges. Because the Swagelok-NPT connection was not sealed by Teflon tape, we determined that it was not airtight and leaked a small amount of argon into the vacuum chamber around the connector. Because the connector was made of steel and was in direct contact with the high-voltage anode, strong electric fields were present around the leaky connection. We believe that these concentrations successfully accelerated free electrons to high speeds and resulted in an initial plasma forming through collisions with leaking argon. The initial plasma itself released high energy electrons capable of causing ionization, and so the initial plasma spark caused a “cascading” ionization effect through which the initial plasma propagated down the propellant feed line and into the thruster channel where a thrust plume formed. The theory that the initial plasma formed at this leaky connection is further evidenced by the fact that later attempts to recreate this result, with Kapton tape insulating all sharp electrically charged components and sealing all tube connectors, failed to generate any plasma. The third flash was white and blue, in contrast with the pink glow of the argon plasma. We suspect that this flash may have been the corona of an electric arc. While the fitting itself was not leaking propellant (evidenced by the facts that a mechanical gas flow valve to the line was closed and that the discharge was not pink), the electric field was likely strong enough to force electrons to jump through free space from the Swagelok fitting on the cathode feed to the grounded baseplate of the thruster stand.

C. Boron Nitride Discoloration

After the successful pulsed firing during test 2, and before conducting test 3, the test chamber was opened and the thruster hardware inspected. One major discovery upon inspection was that the boron nitride on the channel walls was discolored near the exit plane, in the region of peak magnetic field strength. This discoloration is indicative of nominal plasma formation; boron nitride discolors as a response to reaction with plasma, and so the significant discoloration near the exit plane, in the region of the channel where COMSOL predicted peak magnetic field strength, is indicative that plasma successfully formed in that field region and suggests that we both successfully generated and controlled plasma in the channel. An image of this discoloration is given in fig. 15.

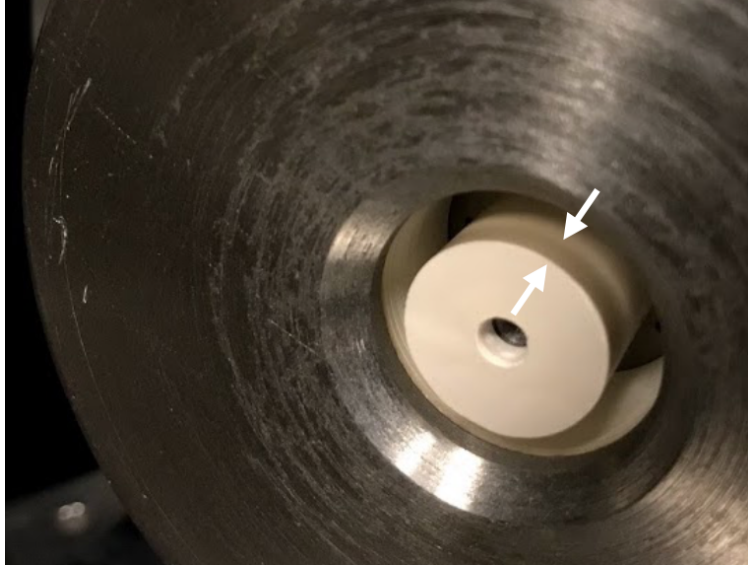


FIG. 15. Photo taken after the successful pulsed firing. Discoloration is visible on the boron nitride inner wall near the exit plane (arrows added), in the region where the magnetic field strength peaks. This discoloration is indicative of plasma formation in intended the region of the channel.

VI. FUTURE ITERATIONS

In the future, our primary goal is to achieve continuous firing. There are two potentially “quick and easy” suggestions that would be our first next steps; the first suggestion, as recommended by two electric propulsion experts at JPL, is to replace the cathode with a bare wire. The hollow cathode is designed to protect the filament by reducing collisions with ions and other energetic particles. This dramatically increases the filament lifetime, but at the expense of complexity, as it requires a hollow cathode to be constructed. However, simply running current through the bare filament, and holding that filament near the thruster channel, could potentially emit enough high energy electrons to cause (and maintain) ignition. The filament will experience dramatic erosion, but this nonetheless serves well for laboratory testing. The second potentially easy variable is the propellant; a quick next step would be to attempt to fire the thruster with a heavier element, such as krypton or xenon, both of which have significantly lower work functions and would be easier to ionize. The major hurdle to this is cost; both krypton and xenon are significantly more expensive than argon and would require additional sources of funding. Beyond these relatively quick steps, the next set of iterations would involve redesigning the thruster to have a larger channel and to

use electromagnets, rather than permanent magnets. Increasing the size of the channel will significantly decrease the number of collisions between energetic particles and the channel walls, potentially freeing a greater number of electrons for ionization and ions for thrust. It has been reasonably verified that HETs are inefficient at small scales, as the channel volume to surface area ratio rapidly decreases as the thruster size decreases, resulting in a higher rate of particle collisions with the channel walls.¹⁰ Furthermore, introducing electromagnets would give a future thruster the ability to throttle the strength of the magnetic field, introducing an easily controllable variable that could prove to be a useful aid in thruster ignition. In future iterations we would also like to be able to collect live data during testing. Temperature data would be enormously helpful in ensuring the thruster is operating within reasonable design parameters. The operating efficiency of the thruster could be determined by collecting current measurements during firing and could be verified by a direct measurement of thrust. The final area of particular interest would be collecting field probe data, both for the electric and magnetic fields within the thruster. This data would allow us to better understand the shapes and behavior of the EM fields during operation.

VII. CONCLUSION

Between September and December of 2018, we were able to surpass our initial expectations, managing to design, manufacture, and fire a small HET without any prior experience in electric propulsion. Across four months, we spent approximately one month conducting background research, one and a half months designing the thruster, and one and a half months manufacturing and testing the system. In doing so we performed self-directed learning across a wide variety of topics; the project provided an opportunity not only to learn principles of electric propulsion, but also to study fundamental physics, as most of the team had not taken formal electricity and magnetism classes nor had experience with plasma physics. It also provided an opportunity to interface with topics not typically covered in undergraduate classrooms, such as EM field shaping and design for manufacturing. For these reasons, we believe our progress despite a lack of prior knowledge demonstrates that electric propulsion is more accessible than is typically considered, both as a field of study and as an educational tool.

Although the thruster did not fire continuously, we still managed to achieve ignition with

only free electrons in the vacuum chamber. In order to better understand our system and attempt to achieve continuous firing, additional work and potential redesign opportunities have surfaced and present a forward course for further investigation. Regardless, as a self-contained experiment we consider the project to have reached a successful conclusion in the light of achieving thruster ignition and steady pulsed firing.

ACKNOWLEDGMENTS

The authors would like to thank Bjarni rn Kristinsson (MIT) for his highly appreciated involvement and assistance throughout the project. We would also like to extend a special thanks to Prof. Paulo Lozano (MIT) for opening the doors of his Space Propulsion Lab at MIT and allowing us to use his laboratory and vacuum chamber for testing. Furthermore, we would like to thank Prof. Manuel Martinez-Sanchez (MIT), Dr. Steve Snyder (JPL), Dr. Dan Goebel (JPL), and Dr. David Oh (JPL) for their time and willingness to accept questions as the project progressed, as well as Dr. James Szabo (Busek) for advice regarding propellant types and boron nitride manufacturing techniques. We would also like to acknowledge Sparsh Bansal (Olin College) and C. Lal Alloys Pvt. Ltd. for donating the material and manufacturing time for many of our thruster components and for serving as consultants as we iterated upon our mechanical design. We are also extremely grateful to Busek Co. for donating the boron nitride stock necessary to manufacture the channel walls.

* Rebecca.Christianson@olin.edu

¹ D. M. Goebel and I. Katz, *Fundamentals of Electric Propulsion: Ion and Hall Thrusters*, JPL Space Science and Technology Series (Jet Propulsion Laboratory, 2008).

² V. Croes, A. Tavant, R. Lucken, R. Martorelli, T. Lafleur, A. Bourdon, and P. Chabert, Physics of Plasmas **25**, 063522 (2018), <https://doi.org/10.1063/1.5033492>.

³ R. Kawashima, J. Bak, K. Komurasaki, and H. Koizumi, Front. Appl. Plasma Technol. , 7 (2018).

⁴ S. E. Cusson, M. P. Georgin, H. C. Dragnea, E. T. Dale, V. Dhaliwal, I. D. Boyd, and A. D. Gallimore, Journal of Applied Physics **123**, 133303 (2018), <https://doi.org/10.1063/1.5028271>.

- ⁵ R. Barry, *The Physics Teacher* **46**, 267 (2008), <https://doi.org/10.1119/1.2909742>.
- ⁶ J. S. Huebner, A. S. Fletcher, J. A. Cato, and J. A. Barrett, *American Journal of Physics* **67**, 1031 (1999), <https://doi.org/10.1119/1.19167>.
- ⁷ D. N. Syarafina, Jailani, and R. Winarni, *AIP Conference Proceedings* **2014**, 020024 (2018), <https://aip.scitation.org/doi/pdf/10.1063/1.5054428>.
- ⁸ M. P. Silverman, *American Journal of Physics* **63**, 495 (1995), <https://doi.org/10.1119/1.18080>.
- ⁹ M. Baird, *Designing an Accessible Hall Effect Thruster*, Senior thesis, Western Michigan University (2016).
- ¹⁰ N. Z. Warner, *Theoretical and Experimental Investigation of Hall Thruster Miniaturization*, Ph.D. thesis, Massachusetts Institute of Technology (2007).
- ¹¹ H.-K. Chung, M. Chen, W. Morgan, Y. Ralchenko, and R. Lee, *High Energy Density Physics* **1**, 3 (2005).
- ¹² K. Takasumi, P. Dent, J. Liu, M. Marinescu, and M. Walmer, in *2009 IEEE International Vacuum Electronics Conference* (2009) pp. 565–566.